

Article

Study of Random Walk Invariants for Spiro-Ring Network Based on Laplacian Matrices

Yasir Ahmad ¹, Umar Ali ², Daniele Ettore Otera ^{3,*} and Xiang-Feng Pan ¹

¹ School of Mathematical Sciences, Anhui University, Hefei 230601, China; yasirahmad6667@gmail.com (Y.A.); xfpan@ahu.edu.cn (X.-F.P.)

² Business School, University of Shanghai for Science and Technology, Shanghai 200093, China; umarali@usst.edu.cn or umarali.msc@gmail.com

³ Institute of Data Science and Digital Technologies, Vilnius University, 08412 Vilnius, Lithuania

* Correspondence: daniele.otera@mif.vu.lt or daniele.otera@gmail.com

Abstract: The use of the global mean first-passage time (GMFPT) in random walks on networks has been widely explored in the field of statistical physics, both in theory and practical applications. The GMFPT is the estimated interval of time needed to reach a state j in a system from a starting state i . In contrast, there exists an intrinsic measure for a stochastic process, known as Kemeny's constant, which is independent of the initial state. In the literature, it has been used as a measure of network efficiency. This article deals with a graph-spectrum-based method for finding both the GMFPT and Kemeny's constant of random walks on spiro-ring networks (that are organic compounds with a particular graph structure). Furthermore, we calculate the Laplacian matrix for some specific spiro-ring networks using the decomposition theorem of Laplacian polynomials. Moreover, using the coefficients and roots of the resulting matrices, we establish some formulae for both GMFPT and Kemeny's constant in these spiro-ring networks.

Keywords: spiro-ring network; random walk; global mean first-passage time; Kemeny's constant

MSC: 05C50; 05C81; 05C92



Citation: Ahmad, Y.; Ali, U.; Otera, D.E.; Pan, X.-F. Study of Random Walk Invariants for Spiro-Ring Network Based on Laplacian Matrices. *Mathematics* **2024**, *12*, 1309. <https://doi.org/10.3390/math12091309>

Academic Editor: Andrea Scozzari

Received: 17 March 2024

Revised: 15 April 2024

Accepted: 23 April 2024

Published: 25 April 2024



Copyright: © 2024 by the authors. Licensee MDPI, Basel, Switzerland. This article is an open access article distributed under the terms and conditions of the Creative Commons Attribution (CC BY) license (<https://creativecommons.org/licenses/by/4.0/>).

1. Introduction

The empirical investigation of real-world networks has inspired many scientists to study complex chemical networks in detail. They have many useful applications in physics and biophysics, as well as in quantum chemistry for molecular modeling, in statistical mechanics for bulk matter properties, and in molecular dynamics simulations for the study of molecular behavior. These networks aid in the understanding of atomic and molecular structures, electronic properties, and fundamental physical origins in various physical contexts of materials science.

Recently, several scientific research fields have shown a particular interest in the study of random walks on complex networks. *Random walks* [1] are stochastic processes characterized by irregular fluctuations, where each step in the process is determined randomly, independently from past events. The mathematical theory of random walks has been widely applied in several domains, such as machine learning [2], optimization [3], artificial intelligence [4], engineering [5], biology [6], physics, and other disciplines [7,8].

In order to motivate our study, which concerns some specific chemical structures called *spiro compounds*, and to provide an explanation of the physical significance and justification behind the spreading processes on spiro-ring networks, we briefly highlight some practical implications and potential real-world applications of our findings, even if our main focus is more in chemistry than in physics. Random walks are often used as essential models in the field of physical systems to describe the probabilistic movement of particles or entities in different media, such as gases, liquids, or solids. To better understand

the connections between the selected structures and physical processes, it is crucial to investigate the fundamental principles and behaviors which lie behind them. This involves exploring the geometric properties, topological arrangements, and dynamic aspects of these formations.

1.1. Global Mean First-Passage Time and the Kemeny Constant

Given a network, the so-called *first-passage time* (FPT) [9] is the estimated time needed by a random walker, starting from an initial point, to reach a particular target point. It represents a sort of metric, associated with a random walk, which helps the understanding of the physical system under observation. On the other hand, the *global mean first-passage time* (GMFPT), denoted also by $\langle T \rangle_g$ (where g stands for ‘global’), is a related valuable tool for analyzing the behavior of random walks, since it describes the average of the FPT’s obtained from all of the source points in the network.

The GMFPT measures the information propagation efficiency, discovery time, and predicted time for a random walker to visit a target node in a network. It is significant in order to measure the capability of transport operations between nodes in the context of a spiro-ring network. For instance, the GMFPT helps to indicate how quickly particles or information can travel between nodes in spiro-ring networks.

It is useful to emphasize the relevance of the GMFPT over other metrics used to analyze system dynamics. In fact, it presents a unique perspective by measuring the average time it takes for a message, particle, or entity to move from one place to another within the system. With this system-wide perspective, the GMFPT may measure the entire efficiency and dynamics of communication or particle movements, allowing research to find bottlenecks, inefficiencies, or preferred paths. Furthermore, its flexibility to varying system parameters, enables its use in a variety of scenarios, making it an effective tool for evaluating a wide range of systems, including networks, stochastic optimization [9], biological processes [10], finance [11], complex network analysis [12], and many others.

On the other hand, another important probabilistic notion directly associated with random walks in graphs and networks, is the *Kemeny constant* (also known as the Kemeny score), denoted by \mathcal{K} . It is a mathematical concept used to rank or order items based on preferences or pairwise comparisons. In the 1950s, Kemeny and Snell [13] established a model that represents the total time-scale associated with relaxation in a Markov chain or kinetic network. In one sentence, the Kemeny constant roughly measures the expected time it takes to go from a randomly chosen state of the network to another randomly chosen one. What is interesting here is that this quantity only depends on the network, and not on the chosen starting state!

The Kemeny constant can be thought of as an indicator of network effectiveness, since it represents the estimated minimum number of steps for a random walk on the network to attain a stationary distribution. It is a helpful statistic to differentiate networks on the basis of their traversal times. Furthermore, the analysis of random walk behavior on a spiro-ring network and the comparison of its characteristics with those of other networks requires the application of the Kemeny constant. It can be used to figure out how information spreads in a spiro-ring network.

The Kemeny constant has also sparked great attention in network research, graph theory, and data analysis. For instance, it is used to compute the Kirchhoff index of graphs, and it is offered as an objective function for optimization in graph clustering algorithms.

1.2. Notation and Definitions

All of the networks and graphs considered in this article are undirected and simple. Let \mathcal{G} be an undirected graph with $|E_{\mathcal{G}}| = m$ and $|V_{\mathcal{G}}| = n$, where $E_{\mathcal{G}}$ and $V_{\mathcal{G}}$ are, respectively, the sets of edges and of vertices of \mathcal{G} . In this study, any standard notation and terminology that are not defined will be as defined in the classical literature, e.g., [14].

Let $D_{\mathcal{G}} = \text{diag}(d_1, \dots, d_{|V_{\mathcal{G}}|})$ be the diagonal matrix representing the vertex degrees, where d_i indicates the degree of the vertex v_i in the graph \mathcal{G} ; and denote by $A_{\mathcal{G}}$ the

adjacency matrix, that is, the square matrix whose entry (i, j) is 1 if v_i is adjacent to v_j , and 0 otherwise. The standard matrix representation of a graph is given by its Laplacian matrix L_G , which may be defined as $D_G - A_G$. The Laplacian matrix is positive semi-definite, and so its eigenvalues can be ordered in an ascending manner, and it turns out that a graph is connected if and only if the first eigenvalue of its Laplacian matrix is zero (see [14]).

In order to evaluate the spread of the signal network, one may use the first-passage time (FPT), that is, the time needed for a random walker to arrive at a target point starting from a given origin in a minimum number of steps. But also the mean first-passage time (MFPT), which is the average time it takes for a diffusing particle to reach a target position for the first time. One area of research investigates just the relationships between the distribution of the MFPT and the structural features of a network. This relationship can be used to improve search efficiency, but it requires prior knowledge of the target. Hence, in the absence of knowledge regarding the target node, the issue of search efficiency becomes a very difficult problem.

The average expected time across all point pairings of a graph \mathcal{G} , represented by $\langle T(\mathcal{G}) \rangle_g$, is referred to as the global mean first-passage time (g stands for global), and it is defined as

$$\langle T(\mathcal{G}) \rangle_g = \frac{1}{|V_G|(|V_G| - 1)} \times \sum_{i \neq j} T_{ij}(\mathcal{G}), \tag{1}$$

where T_{ij} is the number of steps taken for a random walker between nodes i and j .

For a linked network \mathcal{G} with n nodes, Zhu et al. [15] and Gutman and Mohar [16] have separately demonstrated that

$$n \sum_{i=2}^n \frac{1}{\gamma_i} = \sum_{i < j} r_{ij}, \tag{2}$$

where $0 = \gamma_1 < \gamma_2 \leq \gamma_3 \leq \dots \leq \gamma_n$ are the eigenvalues of $L(\mathcal{G})$, and r_{ij} denotes the electric resistance distance between the vertices of the graph \mathcal{G} , namely, the resistance between the two respective vertices of an electrical network corresponding to \mathcal{G} , with the property that the resistance of each bond joining adjacent vertices is 1.

Chandra et al. [17] presented a novel method for a connected graph \mathcal{G} , discovering the following relationship between T_{ij} and r_{ij} :

$$T_{ij} + T_{ji} = 2|E_G| \times r_{ij}. \tag{3}$$

Equation (3) implies, in particular, that $\sum_{i \neq j} T_{ij}(\mathcal{G}) = 2|E_G| \times \sum_{i < j} r_{ij}$.

Therefore, by using all the equations above, we obtain formulae for MFPT:

$$\langle T(\mathcal{G}) \rangle_g = \frac{2|E_G|}{|V_G|(|V_G| - 1)} \times \sum_{i < j} r_{ij} = \frac{2|E_G|}{(|V_G| - 1)} \times \sum_{i=2}^n \frac{1}{\gamma_i} \tag{4}$$

On the other hand the Kemeny constant is given by the following formula (see [18]):

$$\mathcal{K}(\mathbb{S}\mathbb{P}_n) = \sum_{j=2}^n \frac{1}{\gamma_j}, \text{ where, again, } \gamma_j \text{ are the eigenvalues of } L(\mathcal{G}). \tag{5}$$

Remark 1. Note that in both formulae, the first eigenvalue (i.e., for $j = 1$) is zero due to the connectedness of the graph.

In order to give an idea of the importance and use of the Laplacian matrix in practical applications, let us note that Xiao and Gutman [19] established the feasibility of calculating the resistance distance using the eigenvalues of the Laplacian matrix. In 2018, Zhang et al. [20] determined the GMFPT duration of random walks on Vicsek fractals by means of the Laplacian matrix eigenvalues. In [21], Zeman et al. determined the GMFPT and

Kemeny constant of a random walk of pentagonal networks. In 2021, Ali et al. [22,23] obtained the resistance-distance-based indices of linear pentagonal–quadrilateral networks. Topological indices for chemical graph products, carbon nanotubes, and generalized bridge molecular graphs were discussed by Zhang et al. [24]. Finally, the study conducted by Ullah et al. [25] determined degree-based topological indicators for molecular graphs.

In this article, motivated by previous works [26–28], we establish some explicit closed-form formulae for the GMFPT and Kemeny constant in the context of spiro-ring networks, using the Laplacian decomposition theorem. On the basis of the obtained results, comparative studies are carried out for them.

1.3. Spiro-Ring Networks

Spiro compounds represent a fundamental category of cycloalkanes within the field of organic chemistry. They are biologically active organic compounds with a particular structure, that can be found in a wide variety of natural products. More specifically, these compounds consist of two or more rings which have at least one common atom, represented by a cut-vertex in the corresponding molecular graph. A spiro-hexagonal chain $\mathbb{S}\mathbb{P}_n$ is created when a spiro compound consists of hexagonal rings and every cut-vertex is shared by precisely two hexagons. The length of a spiro-hexagonal chain is defined as the number of hexagons it contains. There are different types of substances based on the number of spiro atoms (i.e., the common atoms) they contain, such as monospiro, dispiro, trispiro, and so on. Three straight polyspiro alicyclic hydrocarbons are shown in Figure 1. The basic idea and practical applications of modeling random paths on spiro-ring networks are related in particular to the representation of the structures of spiro compounds in chemistry.

In the present work, we will examine a subcategory of unbranched multispiro molecules whose corresponding graphs are referred to as spiro-hexagonal chains (or chain hexagonal cacti [29], or six-membered ring spiro chains [30]). In particular, these chains, denoted by $\mathbb{S}\mathbb{P}_n$, consist of hexagonal rings, while the corresponding networks have $5n$ nodes and $6n$ edges (see Figure 2).

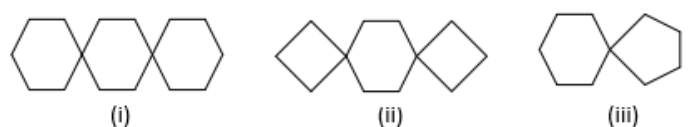


Figure 1. (i) Dispiro[5,2,5]hexadecane, (ii) spiro[4,5]decane, and (iii) dispiro[3,2,3,2]dodecane.

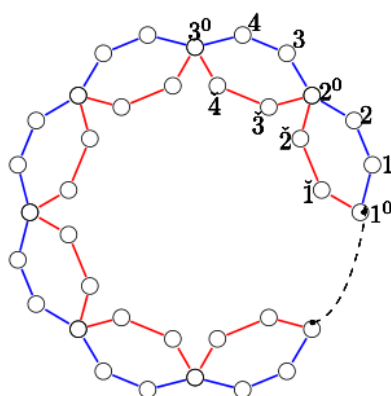


Figure 2. A spiro-ring network $\mathbb{S}\mathbb{P}_n$.

The choice of spiro-ring networks as the subject for our study is inspired by their representation of spiro-compound structures in chemistry. Providing a better understanding of the physical principles underpinning the modeling of random walks on molecular structures gives valuable insights for the fundamental dynamics of molecular systems. Random walks are a key framework used to describe the stochastic movement of particles,

explore structural distance, and study the kinetics of molecular interactions. By revealing the physical intuition and practical implications of modeling random walks on molecular structures, researchers may increase their knowledge of complex systems and propose novel ways for tackling contemporary issues.

Spreading processes, such as disease transmission or information propagation, are complicated phenomena impacted by multiple variables, including network structure, connection, and dynamics. Although spiro-ring-network-based theoretical models could provide insight into certain elements of spreading processes, their relevance to actual situations has to be carefully considered. Constructing physical spiro-ring networks and performing controlled tests to confirm theoretical predictions may offer considerable obstacles owing to the intricate architecture of these networks and the intricacy of spreading processes. Additionally, turning theoretical models into practical applications, such as creating efficient communication networks or forecasting disease outbreaks, needs exacting empirical evidence and validation from empirical data.

2. Main Lemmas

In the present context, and all through the paper, a square matrix B of order n will be represented by its characteristic polynomial $\varphi(B)$, defined as follows: $\varphi(B) = \det(xI_n - B)$. Also, given a graph \mathcal{G} , an automorphism of it will be represented as a permutation π of $V_{\mathcal{G}}$ (the set of vertices of the graph), for which the following property holds: $v_i v_k \in E(\mathcal{G})$ if and only if $\pi(v_j) \pi(v_k)$ is a path in \mathcal{G} (where $E(\mathcal{G})$ is the set of edges of the graph \mathcal{G}). Finally, from now on, we will use the notation $\langle T \rangle_{\mathcal{G}}$ and \mathcal{K} for the global mean first-passage time (GMFPT) and the Kemeny constant, respectively.

Based on the vertex labeling of the spiro-ring network $\mathbb{S}\mathbb{P}_n$ shown in Figure 2, it is clear that $V_{\mathcal{G}}$ can be expressed as the union of three disjoint sets: $V_0 = \{1^0, 2^0, \dots, n^0\}$, $V_1 = \{1, 2, \dots, 2n\}$, and $V_2 = \{\check{1}, \check{2}, \dots, \check{2}n\}$. This means that $|V_{\mathcal{G}}| = 5n$, while $|E_{\mathcal{G}}| = 6n$. It is also obvious that

$$\pi = (1^0)(2^0) \cdots (n^0)(1, \check{1})(2, \check{2}) \cdots (2n, \check{2}n),$$

is an automorphism of $\mathbb{S}\mathbb{P}_n$. Thus, the Laplacian matrix $L(\mathbb{S}\mathbb{P}_n)$ can be represented in the form of the following block matrices:

$$L(\mathbb{S}\mathbb{P}_n) = \begin{pmatrix} L_{V_{00}} & L_{V_{01}} & L_{V_{02}} \\ L_{V_{10}} & L_{V_{11}} & L_{V_{12}} \\ L_{V_{20}} & L_{V_{21}} & L_{V_{22}} \end{pmatrix},$$

where $L_{V_{ik}}$ represents the sub-matrix corresponding to the vertices of V_i and V_k , respectively, where $i, k \in \{0, 1, 2\}$. Further, $L_{V_{11}} = L_{V_{22}}$ thanks to the automorphism of \mathcal{G} associated with π . Let

$$P = \begin{pmatrix} I_n & 0 & 0 \\ 0 & \frac{1}{\sqrt{2}} I_{2n} & \frac{1}{\sqrt{2}} I_{2n} \\ 0 & \frac{1}{\sqrt{2}} I_{2n} & -\frac{1}{\sqrt{2}} I_{2n} \end{pmatrix}$$

be the matrix of blocks whose dimensions are the same as those of the blocks in $L(\mathbb{S}\mathbb{P}_n)$. Then, we have that

$$PL(\mathbb{S}\mathbb{P}_n)P' = \begin{pmatrix} L_R(\mathbb{S}\mathbb{P}_n) & 0 \\ 0 & L_S(\mathbb{S}\mathbb{P}_n) \end{pmatrix},$$

where P' represents the transpose of P ,

$$L_R(\mathbb{S}\mathbb{P}_n) = \begin{pmatrix} L_{V_{00}} & \sqrt{2}L_{V_{01}} \\ \sqrt{2}L_{V_{10}} & L_{V_{11}} + L_{V_{12}} \end{pmatrix}, \text{ and } L_S(\mathbb{S}\mathbb{P}_n) = L_{V_{11}} - L_{V_{12}}. \tag{6}$$

The Laplacian polynomial decomposition theorem is expressed by the following lemma:

Lemma 1 ([31]). Assume that $L_R(\mathbb{S}\mathbb{P}_n)$ and $L_S(\mathbb{S}\mathbb{P}_n)$ are the matrices described above. Then,

$$\varphi(L(\mathbb{S}\mathbb{P}_n)) = \varphi(L_R(\mathbb{S}\mathbb{P}_n)) \cdot \varphi(L_S(\mathbb{S}\mathbb{P}_n)).$$

In accordance with Lemma 1, we initially determine the eigenvalues of the Laplacian for $\mathbb{S}\mathbb{P}_n$. Subsequently, we will provide the formula for the summation of the reciprocal and products of the eigenvalues of the Laplacian. This formulation serves as the motivation for calculating \mathcal{K} and $\langle T(\mathcal{G}) \rangle_g$. According to the structure of Figure 2, we obtain that $L_{V_{00}} = 4I_n$ and $L_{V_{12}} = O_{2n \times 2n}$. So, $L_{V_{01}}$ and $L_{V_{11}}$ are matrices of sizes $n \times (2n)$ and $(2n) \times (2n)$, respectively, as shown below:

$$L_{V_{01}} = \begin{pmatrix} -1 & 0 & 0 & 0 & 0 & \cdots & -1 \\ 0 & -1 & -1 & 0 & 0 & \cdots & 0 \\ 0 & 0 & 0 & -1 & -1 & \cdots & 0 \\ \vdots & \vdots & \vdots & \vdots & \vdots & \ddots & \vdots \\ 0 & 0 & 0 & 0 & 0 & \cdots & 0 \end{pmatrix}, \text{ and } L_{V_{11}} = \begin{pmatrix} 2 & -1 & 0 & 0 & \cdots & 0 & 0 \\ -1 & 2 & 0 & 0 & \cdots & 0 & 0 \\ 0 & 0 & 2 & -1 & \cdots & 0 & 0 \\ 0 & 0 & -1 & 2 & \cdots & 0 & 0 \\ \vdots & \vdots & \vdots & \vdots & \ddots & \vdots & \vdots \\ 0 & 0 & 0 & 0 & \cdots & 2 & -1 \\ 0 & 0 & 0 & 0 & \cdots & -1 & 2 \end{pmatrix}_{2n \times 2n}.$$

Therefore,

$$L_R = \begin{pmatrix} 4 & 0 & 0 & \cdots & 0 & -\sqrt{2} & 0 & 0 & 0 & 0 & \cdots & -\sqrt{2} \\ 0 & 4 & 0 & \cdots & 0 & 0 & -\sqrt{2} & -\sqrt{2} & 0 & 0 & \cdots & 0 \\ 0 & 0 & 4 & \cdots & 0 & 0 & 0 & 0 & -\sqrt{2} & -\sqrt{2} & \cdots & 0 \\ \vdots & \vdots & \vdots & \ddots & \vdots & \vdots & \vdots & \vdots & \vdots & \vdots & \ddots & \vdots \\ 0 & 0 & 0 & \cdots & 4 & 0 & 0 & 0 & 0 & 0 & \cdots & 0 \\ -\sqrt{2} & 0 & 0 & \cdots & 0 & 2 & -1 & 0 & 0 & 0 & \cdots & 0 \\ 0 & -\sqrt{2} & 0 & \cdots & 0 & -1 & 2 & 0 & 0 & 0 & \cdots & 0 \\ 0 & -\sqrt{2} & 0 & \cdots & 0 & 0 & 0 & 2 & -1 & 0 & \cdots & 0 \\ 0 & 0 & -\sqrt{2} & \cdots & 0 & 0 & 0 & -1 & 2 & 0 & \cdots & 0 \\ 0 & 0 & -\sqrt{2} & \cdots & 0 & 0 & 0 & 0 & 0 & 2 & \cdots & 0 \\ \vdots & \vdots & \vdots & \ddots & \vdots & \vdots & \vdots & \vdots & \vdots & \vdots & \ddots & \vdots \\ -\sqrt{2} & 0 & 0 & \cdots & 0 & 0 & 0 & 0 & 0 & 0 & \cdots & 2 \end{pmatrix}_{3n \times 3n},$$

and $L_S = L_{V_{11}}$.

The matrix determinant lemma can be used in order to calculate the determinant of a square matrix of a rank-one perturbation.

Lemma 2 ([32]). Let H_{11} , H_{12} , H_{21} , and H_{22} be matrices of orders $n \times m$, $n \times n$, $m \times n$, and $m \times m$, respectively. Assume that H_{22} is invertible. Then,

$$\det \begin{pmatrix} H_{11} & H_{12} \\ H_{21} & H_{22} \end{pmatrix} = \det(H_{22}) \cdot \det(H_{11} - H_{12}H_{22}^{-1}H_{21}),$$

and $H_{11} - H_{12}H_{22}^{-1}H_{21}$ is called the Schur complement of H_{22} .

3. Kemeny’s Constant and the GMFPT of Spiro-Ring Networks

Spiro-ring networks, known for their hexagonal configuration of interconnected nodes in a spiral pattern, are widely used in several fields due to their specific topology and features. Thanks to their distinctive topology, with a spiral arrangement of interconnected nodes, they have various applications. Researchers can use the implications of the GMFPT and the Kemeny constant to make informed choices that improve the reliability, efficiency, and scalability of spiro-ring networks in many areas, like telecommunications, transporta-

As a result, we have proved Proposition 2.

Proposition 3. Assume that $0 = \phi_1 < \phi_2 \leq \dots \leq \phi_{3n}$ are the eigenvalues of L_R . Then, we have that $\sum_{j=2}^{3n} \frac{1}{\phi_j} = \frac{75n^2-11}{120}$.

Proof. As before, let $\varphi(L_R) = x^{3n} + b_1x^{3n-1} + \dots + b_{3n-2}x^2 + b_{3n-1}x$ be the characteristic polynomial. We can precisely determine $\phi_2, \phi_3, \dots, \phi_{3n}$ as the roots of the equation: $x^{3n-1} + b_1x^{3n-2} + \dots + b_{3n-2}x + b_{3n-1} = 0$. From Vieta’s formula, we have

$$\sum_{j=2}^{3n} \frac{1}{\phi_j} = -\frac{b_{3n-2}}{b_{3n-1}}. \tag{8}$$

□

The following two lemmas specify the expressions for b_{3n-2} and b_{3n-1} , respectively.

Lemma 4. $b_{3n-1} = (-1)^{n-1} \frac{15}{2} \cdot n^2 2^n$.

Proof. Refer to the Appendix A for the proof. □

Lemma 5. $b_{3n-2} = (-1)^n 2^n \frac{15(75n^4-11n^2)}{16}$.

Proof. Refer to the Appendix A for the proof. As a result, we have proved Proposition 3. □

Theorem 1. Let \mathbb{SP}_n be a spiro-ring network of length n (i.e., with n hexagons) and denote by \mathcal{K} its Kemeny’s constant. Then,

$$\mathcal{K}(\mathbb{SP}_n) = \frac{75n^2 + 160n - 11}{120}.$$

Proof. Putting together Propositions 2 and 3 in the formula from Proposition 1, we obtain the desired result. □

Theorem 2. Let $\langle T(\mathbb{SP}_n) \rangle_g$ represent the GMFPT of \mathbb{SP}_n (a spiro-ring network of length n). Then,

$$\langle T(\mathbb{SP}_n) \rangle_g = \frac{12}{5(5n-1)} \left(\frac{75n^2 + 160n - 11}{120} \right).$$

Proof. Putting together Propositions 2 and 3 in Equation (4), and noting that $|E_{\mathbb{SP}_n}| = 6n$, the desired result follows easily. □

In order to overcome any potential limitations of the graph spectrum method, we used the decomposition theorem of Laplacian polynomials to compute the Laplacian matrix, GMFPT, and Kemeny’s constant for spiro-ring networks. This methodology enabled us to surpass the constraints of the graph spectrum method by integrating supplementary mathematical tools to obtain more precise analysis and outcomes.

Comparison

In this section, we present graphical representations of the relationship between Kemeny’s constant \mathcal{K} and GMFPT $\langle T \rangle_g$. The results obtained in Theorems 1 and 2 suggest that, within the network scales under consideration, there exists a linear and direct proportional connection between the quantities $\mathcal{K}(\mathbb{SP}_n)$ and $\langle T(\mathbb{SP}_n) \rangle_g$ as n varies. Our exact

results are confirmed in Figure 3a,b, which indicate how $\mathcal{K}(\mathbb{SP}_n)$ and $\langle T(\mathbb{SP}_n) \rangle_g$ rises as the value of n increases. Similarly, in Figure 4, we just compare $\mathcal{K}(\mathbb{SP}_n)$ and $\langle T(\mathbb{SP}_n) \rangle_g$. Our analysis presents some fresh perspectives that make it simple to identify the structure of our network.

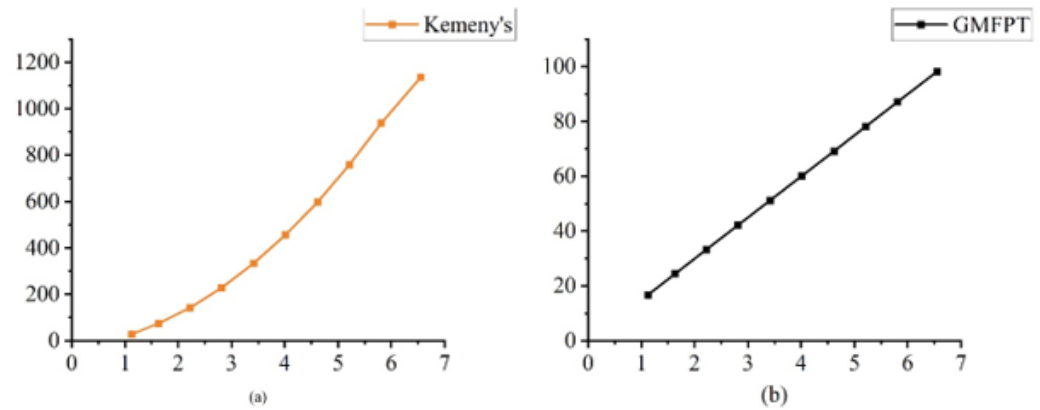


Figure 3. (a) Kemeny's constant $\mathcal{K}(\mathbb{SP}_n)$ and (b) GMFPT $\langle T(\mathbb{SP}_n) \rangle_g$.

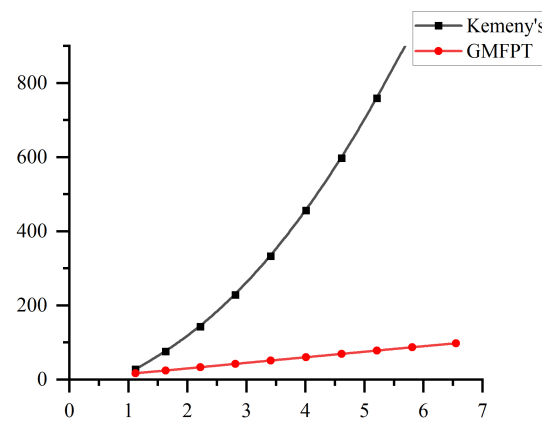


Figure 4. Comparison of $\mathcal{K}(\mathbb{SP}_n)$ and $\langle T(\mathbb{SP}_n) \rangle_g$.

The comparison study of Kemeny's constant and the GMFPT entails the examination of resulting metrics to evaluate the network efficiency, navigability, robustness, and scalability. The GMFPT gives insight into the average time it takes for objects to traverse the spiro-ring network, which is useful for assessing the overall network efficiency. Researchers can evaluate the impact of various network configurations or characteristics on the network efficiency and navigability by comparing the resulting matrices of the GMFPT and the Kemeny constant. These comparative studies offer useful insights into the efficiency and features of spiro-ring networks (see also Figure 5). They inform the design of networks, optimization methodologies, and decision-making processes to improve network efficacy in different applications.

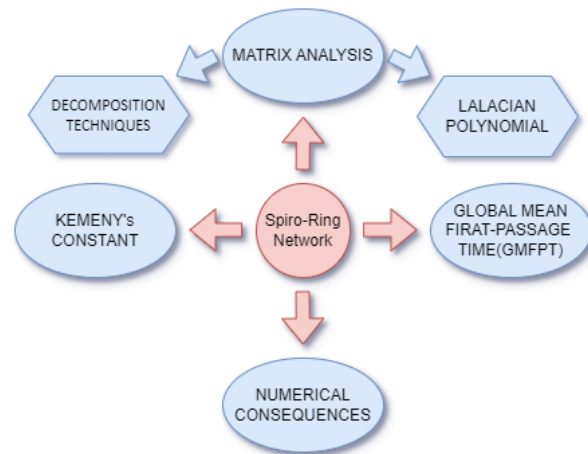


Figure 5. Comparative graph with existing spiro techniques.

4. Conclusions

In the present study, we have dealt with the analysis of some important quantities for spiro-ring networks $\mathbb{S}\mathbb{P}_n$ that are very relevant in network theory. For instance, the famous Kemeny constant \mathcal{K} is a significant and valuable quantifier that finds several applications in a wide range of topics, particularly within the realm of Markov chains; whereas the GMFPT (global mean first-passage time) is the average of the mean first-passage times over the starting point of the walker, and it is considered as a quantitative indicator of the transport efficiency of a network.

In this paper, we emphasize the importance of employing the Laplacian matrix when analyzing graph structures, specifically when performing operations like partitioning a graph into communities or clusters. We demonstrate that the Laplacian matrix's eigenvalues provide useful insights into different elements of a graph, such as its connectivity qualities, spectrum, and the behavior of random walks inside the network. The Laplacian matrix is a powerful tool that may be utilized to analyze the intricate architecture of complex networks, such as social networks, transportation networks, and biological networks.

For instance, through the utilization of the spectra of the Laplacian of $\mathbb{S}\mathbb{P}_n$, precise closed-form formulae have been established both for the GMFPT and \mathcal{K} for $\mathbb{S}\mathbb{P}_n$ networks. Finally, we performed a graphic comparison between them. The results derived from this study will be useful for further investigations in the field of network science.

Research in the field of deterministic structures is both relevant and intriguing due to the significant advancements in supramolecular experimental methods, which enable the chemical synthesis of a wide range of polymers with controlled molecular architectures, including molecular fractals. These models could assist in chemistry by providing insight into solvent effects, molecule binding, and reaction kinetics, which can then be used to develop novel materials or catalysts. Random walk models are used in biophysics to clarify the processes of molecular transport inside cells, the folding dynamics of proteins, and the building of biomolecular complexes. Furthermore, the ideas described in studies of spreading processes on spiro-ring networks could be applied to random graph models defined by blocked structures, such as the stochastic block model (SBM). The SBM is a widely used probabilistic model for modeling networks with a community structure, where nodes are divided into blocks or communities with dense connections inside blocks and sparser connections between blocks. Furthermore, expanding the research to blocked structures allows for the examination of other aspects that may affect spreading processes, such as the number and density of communities, the strength of inter-community linkages, and the existence of overlapping communities.

$$\begin{aligned}
 &= \begin{pmatrix} -\frac{3}{2} & 1 & 0 & 0 & \cdots & 0 & 0 & 0 & 0 & \cdots & 0 \\ 1 & -\frac{3}{2} & \frac{1}{2} & 0 & \cdots & 0 & 0 & 0 & 0 & \cdots & 0 \\ 0 & \frac{1}{2} & -\frac{3}{2} & 1 & \cdots & 0 & 0 & 0 & 0 & \cdots & 0 \\ \vdots & \vdots & \vdots & \vdots & \ddots & \vdots & \vdots & \vdots & \vdots & \ddots & \vdots \\ 0 & 0 & 0 & 0 & \cdots & -2 & 0 & 0 & 0 & \cdots & 0 \\ 0 & 0 & 0 & 0 & \cdots & 0 & -2 & 1 & 0 & \cdots & 0 \\ 0 & 0 & 0 & 0 & \cdots & 0 & 0 & -\frac{3}{2} & \frac{1}{2} & \cdots & 0 \\ 0 & 0 & 0 & 0 & \cdots & 0 & 0 & \frac{1}{2} & -\frac{3}{2} & \cdots & 0 \\ \vdots & \vdots & \vdots & \vdots & \ddots & \vdots & \vdots & \vdots & \vdots & \ddots & \vdots \\ 0 & 0 & 0 & 0 & \cdots & 0 & 0 & 0 & 0 & \cdots & -\frac{3}{2} \end{pmatrix} + \frac{1}{2}e_1e_{2n}^T + \frac{1}{2}e_{2n}e_1^T \\
 &= \begin{pmatrix} C_{2j-2} & 0 \\ 0 & C_{2n-2j+2} \end{pmatrix} + \frac{1}{2}e_1e_{2n}^T + \frac{1}{2}e_{2n}e_1^T \text{ (see Lemma A3).}
 \end{aligned}$$

Since, $\det\left(\begin{pmatrix} C_{2j-2} & 0 \\ 0 & C_{2n-2j+2} \end{pmatrix} + \frac{1}{2}e_1e_{2n}^T\right) = \det\begin{pmatrix} C_{2j-2} & 0 \\ 0 & C_{2n-2j+2} \end{pmatrix}$,

$$\begin{aligned}
 \det\left(\chi + \frac{1}{2}L_{V_{01}}(\{j|\{j}\})^T L_{V_{01}}(\{j|\{j}\})\right) &= \det(C_{2j-2}) \cdot \det(C_{2n-2j+2}) \\
 &+ (-1)^{2n+1} \frac{1}{2} \cdot \frac{1}{2} \det(C_{2j-3}) \cdot \det(C_{2n-2j+1}) \\
 &= \left(\frac{1}{2}\right)^n 6n.
 \end{aligned}$$

Therefore, $\det\left(\chi + \frac{1}{2}L_{V_{01}}(\{j|\{j}\})^T L_{V_{01}}(\{j|\{j}\})\right) = \left(\frac{1}{2}\right)^n 6n$, for $1 \leq j \leq n$.

Case A2. Take the case when $n + 1 \leq j \leq 3n$, let $r = j - n$, we have

$$\det(-L_R(\{r|\{r}\})) = \begin{vmatrix} -4I_n & -\sqrt{2}L_{V_{01}}(\{r|\{r}\}) \\ -\sqrt{2}L_{V_{01}}(\{r|\{r}\})^T & \chi(\{r|\{r}\}) \end{vmatrix} = \begin{vmatrix} -4I_n & 0 \\ 0 & \mathfrak{R}_1 \end{vmatrix},$$

where $\mathfrak{R}_1 = \chi(\{r|\{r}\}) + \frac{1}{2}L_{V_{01}}(\{r|\{r}\})^T L_{V_{01}}(\{r|\{r}\})$ and $\chi = -L_{V_{11}}$. Apply Lemma 2, $-4I_n$ in the preceding determinant, we have $\det(-L_R(\{r|\{r}\})) = \det(-4I_n) \cdot \det(\mathfrak{R}_1)$, for $r = 1, 2, \dots, 2n$. To estimate $\det(\mathfrak{R}_1)$, the following subcases need our attention:

Subcase 2(a): If $1 \leq r \leq 2n$,

$$\begin{aligned}
 \mathfrak{R}_1 &= \chi(\{r|\{r}\}) + \frac{1}{2}L_{V_{01}}(\{r|\{r}\})^T L_{V_{01}}(\{r|\{r}\}) \\
 &= \begin{pmatrix} -\frac{3}{2} & 1 & 0 & 0 & \cdots & 0 & 0 & 0 & 0 & \cdots & \frac{1}{2} \\ 1 & -\frac{3}{2} & \frac{1}{2} & 0 & \cdots & 0 & 0 & 0 & 0 & \cdots & 0 \\ 0 & \frac{1}{2} & -\frac{3}{2} & 1 & \cdots & 0 & 0 & 0 & 0 & \cdots & 0 \\ \vdots & \vdots & \vdots & \vdots & \ddots & \vdots & \vdots & \vdots & \vdots & \ddots & \vdots \\ 0 & 0 & 0 & 0 & \cdots & -\frac{3}{2} & 0 & 0 & 0 & \cdots & 0 \\ 0 & 0 & 0 & 0 & \cdots & 0 & -\frac{3}{2} & \cdots & 0 & 0 & 0 \\ \vdots & \vdots & \vdots & \vdots & \ddots & \vdots & \vdots & \ddots & \vdots & \ddots & \vdots \\ 0 & 0 & 0 & 0 & \cdots & 0 & 0 & \cdots & -\frac{3}{2} & \frac{1}{2} & 0 \\ 0 & 0 & 0 & 0 & \cdots & 0 & 0 & \cdots & \frac{1}{2} & -\frac{3}{2} & 1 \\ \frac{1}{2} & 0 & 0 & 0 & \cdots & 0 & 0 & \cdots & 0 & 1 & -\frac{3}{2} \end{pmatrix}_{2n-1 \times 2n-1} \\
 &= \begin{pmatrix} -\frac{3}{2} & 1 & 0 & 0 & \cdots & 0 & 0 & 0 & 0 & \cdots & 0 \\ 1 & -\frac{3}{2} & \frac{1}{2} & 0 & \cdots & 0 & 0 & 0 & 0 & \cdots & 0 \\ 0 & \frac{1}{2} & -\frac{3}{2} & 1 & \cdots & 0 & 0 & 0 & 0 & \cdots & 0 \\ \vdots & \vdots & \vdots & \vdots & \ddots & \vdots & \vdots & \vdots & \vdots & \ddots & \vdots \\ 0 & 0 & 0 & 0 & \cdots & -\frac{3}{2} & 0 & 0 & 0 & \cdots & 0 \\ 0 & 0 & 0 & 0 & \cdots & 0 & -\frac{3}{2} & \cdots & 0 & 0 & 0 \\ \vdots & \vdots & \vdots & \vdots & \ddots & \vdots & \vdots & \ddots & \vdots & \ddots & \vdots \\ 0 & 0 & 0 & 0 & \cdots & 0 & 0 & \cdots & -\frac{3}{2} & \frac{1}{2} & 0 \\ 0 & 0 & 0 & 0 & \cdots & 0 & 0 & \cdots & \frac{1}{2} & -\frac{3}{2} & 1 \\ 0 & 0 & 0 & 0 & \cdots & 0 & 0 & \cdots & 0 & 1 & -\frac{3}{2} \end{pmatrix} + \frac{1}{2}e_1e_{2n-1}^T + \frac{1}{2}e_{2n-1}e_1^T
 \end{aligned}$$

$$\begin{aligned}
 &= \begin{pmatrix} A_{r-1} & 0 \\ 0 & A_{2n-r} \end{pmatrix} + \frac{1}{2}e_1e_{2n-1}^T + \frac{1}{2}e_{2n-1}e_1^T \text{ (see Lemma A1)} \\
 &= \chi_1 + \frac{1}{2}e_{2n-1}e_1^T, \text{ where } \chi_1 = \begin{pmatrix} A_{r-1} & 0 \\ 0 & A_{2n-r} \end{pmatrix}.
 \end{aligned}$$

Since $\det(\chi_1 + \frac{1}{2}e_1e_{2n-1}^T) = \det(\chi_1) = \det(A_{r-1}) \cdot \det(A_{2n-r})$, then we have that

$$\begin{aligned}
 &\det\left(\chi_1 + \frac{1}{2}e_1e_{2n-1}^T + \frac{1}{2}e_{2n-1}e_1^T\right) = \\
 &\det\left(\chi_1 + \frac{1}{2}e_1e_{2n-1}^T\right) + \frac{1}{2}e_1^T \cdot \text{adj}\left(\chi_1 + \frac{1}{2}e_1e_{2n-1}^T\right) \cdot e_{2n-1} = \\
 &\begin{cases} \det(\chi_1) + (-1)^{2n-1} \frac{\det(A_{r-2}) \cdot \det(D_{2n-r-1})}{4}, & \text{if } r = \text{odd;} \\ \det(\chi_1) + (-1)^{2n-1} \frac{\det(A_{2n-r-1}) \cdot \det(D_{r-2})}{4}, & \text{if } r = \text{even.} \end{cases} \\
 &= -\left(\frac{1}{2}\right)^n 3n.
 \end{aligned}$$

Subcase 2(b): If $r = 2n$, then:

$$\begin{aligned}
 \det\left(\chi(\{r|\{r\}) + \frac{1}{2}L_{V_{01}}(\{r|\{r\})^T L_{V_{01}}(\{r|\{r\})\right) &= \det(A_{2n-1}) \\
 &= -\left(\frac{1}{2}\right)^n 3n.
 \end{aligned}$$

Therefore, for $1 \leq r \leq 2n$, i.e., for $n + 1 \leq j \leq 3n$, one has

$$\det\left(\chi(\{r|\{r\}) + \frac{1}{2}L_{V_{01}}(\{r|\{r\})^T L_{V_{01}}(\{r|\{r\})\right) = -\left(\frac{1}{2}\right)^n 3n.$$

So,

$$\begin{aligned}
 \alpha_{3n-1} &= \sum_{j=1}^{3n} \det(-L_R(\{j|\{j\})) \\
 &= \sum_{j=1}^n \det\left(-L_R(\{j|\{j\})\right) + \sum_{j=n+1}^{3n} \det\left(-L_R(\{j|\{j\})\right) \\
 &= \sum_{j=1}^n (-4)^{n-1} \cdot \left(\frac{1}{2}\right)^n 6n + \sum_{j=n+1}^{3n} (-4)^n \cdot (-1) \left(\frac{1}{2}\right)^n 3n \\
 &= (-1)^{n-1} 2^{n-1} \cdot 15n^2. \quad \square
 \end{aligned}$$

Proof of Lemma 5. Denote by $\mathfrak{B}(\{j, k|\{j, k\})$ the sub-matrix of the matrix \mathfrak{B} after deleting the j th and k th rows and their corresponding columns. Thus,

$$\begin{aligned}
 \alpha_{3n-2} &= \sum_{1 \leq j < k \leq 3n} \det(-L_R(\{j, k|\{j, k\})) \\
 &= \left(\sum_{1 \leq j < k \leq n} + \sum_{n+1 \leq j < k \leq 3n} + \sum_{\substack{1 \leq j \leq n \\ n+1 \leq k \leq 3n}} \right) \det(-L_R(\{j, k|\{j, k\})).
 \end{aligned}$$

Therefore, we evaluate the subsequent cases.

Case A3. Take the case if $1 \leq j \leq n$,

$$\det(-L_R(\{j, k\}|\{j, k\})) = \begin{vmatrix} -4I_{n-2} & -\sqrt{2}L_{V_{01}}(\{j, k\}|\{\}) \\ -\sqrt{2}L_{V_{01}}(\{j, k\}|\{\})^T & \chi \end{vmatrix}, \text{ where } \chi = -L_{V_{11}}.$$

Now, we have the subcases listed below.

Subcase 3.1: If $j = 1$ and $2 \leq k \leq n$, apply the Schur complement, we have

$$\begin{aligned} \det\left(\chi + \frac{1}{2}L_{V_{01}}(\{j, k\}|\{j, k\})^T L_{V_{V_{01}}}(\{j, k\}|\{j, k\})\right) &= \begin{vmatrix} R_{2k-2} & 0 \\ 0 & R_{2n-2k+2} \end{vmatrix} \\ &= \det(R_{2k-2}) \cdot \det(R_{2n-2k+2}) \\ &= \left(\frac{1}{2}\right)^n 36(k-j)(n-k+1). \end{aligned}$$

Subcase 3.2: If $1 < j < k \leq n$, $R' = \chi + \frac{1}{2}L_{V_{01}}(\{j, k\}|\{j, k\})^T L_{V_{V_{01}}}(\{j, k\}|\{j, k\})$

$$\begin{aligned} &= \begin{pmatrix} -\frac{3}{2} & 1 & 0 & 0 & \dots & 0 & 0 & 0 & 0 & \dots \\ 0 & 0 & 0 & 0 & 0 & \dots & 0 & \frac{1}{2} & 0 & \dots \\ 1 & -\frac{3}{2} & \frac{1}{2} & 0 & \dots & 0 & 0 & 0 & 0 & \dots \\ 0 & 0 & 0 & 0 & 0 & \dots & 0 & 0 & 0 & \dots \\ 0 & \frac{1}{2} & -\frac{3}{2} & 1 & \dots & 0 & 0 & 0 & 0 & \dots \\ 0 & 0 & 0 & 0 & 0 & \dots & 0 & 0 & 0 & \dots \\ \vdots & \vdots & \vdots & \vdots & \ddots & \vdots & \vdots & \vdots & \vdots & \ddots \\ \vdots & \vdots & \vdots & \vdots & \vdots & \ddots & \vdots & \vdots & \vdots & \ddots \\ 0 & 0 & 0 & 0 & \dots & -2 & 0 & 0 & 0 & \dots \\ 0 & 0 & 0 & 0 & 0 & \dots & 0 & 0 & 0 & \dots \\ 0 & 0 & 0 & 0 & \dots & 0 & -2 & 1 & 0 & \dots \\ 0 & 0 & 0 & 0 & 0 & \dots & 0 & 0 & 0 & \dots \\ 0 & 0 & 0 & 0 & \dots & 0 & 1 & -\frac{3}{2} & \frac{1}{2} & \dots \\ 0 & 0 & 0 & 0 & 0 & \dots & 0 & 0 & 0 & \dots \\ 0 & 0 & 0 & 0 & \dots & 0 & 0 & \frac{1}{2} & -\frac{3}{2} & \dots \\ 0 & 0 & 0 & 0 & 0 & \dots & 0 & 0 & 0 & \dots \\ \vdots & \vdots & \vdots & \vdots & \ddots & \vdots & \vdots & \vdots & \vdots & \ddots \\ \vdots & \vdots & \vdots & \vdots & \vdots & \ddots & \vdots & \vdots & \vdots & \ddots \\ 0 & 0 & 0 & 0 & \dots & 0 & 0 & 0 & 0 & \dots \\ -\frac{3}{2} & 1 & 0 & 0 & 0 & \dots & 0 & 0 & 0 & \dots \\ 1 & -2 & 0 & 0 & 0 & \dots & 0 & 0 & 0 & \dots \\ 0 & 0 & 0 & 0 & \dots & 0 & 0 & 0 & 0 & \dots \\ 0 & 0 & -2 & 1 & 0 & \dots & 0 & 0 & 0 & \dots \\ 0 & 0 & 0 & 0 & \dots & 0 & 0 & 0 & 0 & \dots \\ 0 & 0 & 1 & -\frac{3}{2} & \frac{1}{2} & \dots & 0 & 0 & 0 & \dots \\ 0 & 0 & 0 & 0 & \dots & 0 & 0 & 0 & 0 & \dots \\ 0 & 0 & 0 & \frac{1}{2} & -\frac{3}{2} & \dots & 0 & 0 & 0 & \dots \\ \vdots & \vdots & \vdots & \vdots & \ddots & \vdots & \vdots & \vdots & \vdots & \ddots \\ \vdots & \vdots & \vdots & \vdots & \vdots & \ddots & \vdots & \vdots & \vdots & \ddots \\ 0 & 0 & 0 & 0 & \dots & 0 & 0 & 0 & 0 & \dots \\ 0 & 0 & 0 & 0 & 0 & \dots & -\frac{3}{2} & 1 & 0 & \dots \\ \frac{1}{2} & 0 & 0 & 0 & \dots & 0 & 0 & 0 & 0 & \dots \\ 0 & 0 & 0 & 0 & 0 & \dots & 1 & -\frac{3}{2} & 0 & \dots \end{pmatrix} \\ &= \begin{pmatrix} C_{2j-2} & 0 & 0 \\ 0 & R_{2k-2j} & 0 \\ 0 & 0 & C_{2n-2k+2} \end{pmatrix} + \frac{1}{2}e_1e_{2n}^T + \frac{1}{2}e_{2n}e_1^T. \end{aligned}$$

Now, $\det \left[\begin{pmatrix} C_{2j-2} & 0 & 0 \\ 0 & R_{2k-2j} & 0 \\ 0 & 0 & C_{2n-2k+2} \end{pmatrix} + \frac{1}{2} e_1 e_{2n}^T \right] = \det(C_{2j-2}) \det(R_{2k-2j}) \det(C_{2n-2k+2})$. Then,

$$\begin{aligned} \det(R') &= \det(C_{2j-2}) \det(R_{2k-2j}) \det(C_{2n-2k+2}) \\ &+ (-1)^{2n+1} \frac{1}{4} \det(C_{2j-3}) \cdot \det(C_{2n-2k+1}) \\ &= \left(\frac{1}{2}\right)^n 36(k-j)(n-k+1). \end{aligned}$$

So, if $1 \leq j < k \leq n$,

$$\begin{aligned} \sum_{1 \leq j < k \leq n} \det(-L_R(\{j, k\}|\{j, k\})) &= (-4)^{n-2} \sum_{1 \leq j < k \leq n} \left(\frac{1}{2}\right)^n 36(k-j)(n-k+1) \\ &= (-4)^{n-2} \left(\frac{1}{2}\right)^n 3n^2(n-1)(n+1). \end{aligned}$$

Case A4. Consider the case when $n + 1 \leq j < k \leq 3n$,

$$\det(-L_R(\{j, k\}|\{j, k\})) = \begin{vmatrix} -4I_n & -\sqrt{2}L_{V_{01}}(\{j\}|\{j, k\}) \\ -\sqrt{2}L_{V_{01}}(\{j\}|\{j, k\})^T & \chi(\{j, k\}|\{j, k\}) \end{vmatrix} = \begin{vmatrix} -4I_n & 0 \\ 0 & \mathfrak{R}_4 \end{vmatrix},$$

where $\mathfrak{R}_4 = \chi(\{j, k\}|\{j, k\}) + \frac{1}{2}L_{V_{01}}(\{j\}|\{j, k\})^T L_{V_{01}}(\{j\}|\{j, k\})$ and $\chi = -L_{V_{11}}$.

$$\det(-L_R(\{j, k\}|\{j, k\})) = \det(-4I_n) \det(\mathfrak{R}_4).$$

Let $r = j - n$ and $t = k - n$. We must examine the next subcases.

Subcase 4.1: $1 < r < t < 2n$, r -even and t -odd or r and t are both odd or both even, we have

$$\mathfrak{R}_4 = \begin{pmatrix} A_{r-1} & 0 & \frac{1}{2}e_1 e_{2n}^T \\ 0 & A_{t-r-1} & 0 \\ \frac{1}{2}e_{2n} e_1^T & 0 & A_{2n-t} \end{pmatrix}.$$

Subcase 4.2: $1 < r < t < 2n$, r -odd and t -even, so

$$\mathfrak{R}_4 = \begin{pmatrix} A_{r-1} & 0 & \frac{1}{2}e_1 e_{2n}^T \\ 0 & D_{t-r-1} & 0 \\ \frac{1}{2}e_{2n} e_1^T & 0 & A_{2n-t} \end{pmatrix}.$$

Subcase 4.3: $r = 1$, $1 < t < 2n$, and t even, we have

$$\mathfrak{R}_4 = \begin{pmatrix} D_{t-2} & 0 \\ 0 & A_{2n-t} \end{pmatrix}.$$

Subcase 4.4: $r = 1$, $1 < t < 2n$, and t -odd, we have

$$\mathfrak{R}_4 = \begin{pmatrix} A_{t-2} & 0 \\ 0 & A_{2n-t} \end{pmatrix}.$$

Subcase 4.5: $1 < r < 2n$, $r = 2n$, and r -even, we have

$$\mathfrak{R}_4 = \begin{pmatrix} A_{r-1} & 0 \\ 0 & A_{2n-r-1} \end{pmatrix}.$$

Subcase 4.6: $1 < r < 2n$, $r = 2n$, and r -odd, we have

$$\mathfrak{R}_4 = \begin{pmatrix} A_{r-1} & 0 \\ 0 & D_{2n-r-1} \end{pmatrix}.$$

As previously, we can proceed as follows:

$$\chi(\{j, k\}|\{j, k\}) + \frac{1}{2}L_{V_{01}}(\{j\}|\{j, k\})^T L_{V_{01}}(\{j\}|\{j, k\}) = \begin{cases} 9\left(\frac{1}{2}\right)^{n+2}(t-r)(2n-t+r), & \text{if } \{r, t\} \text{ are both even or both odd;} \\ \left(\frac{1}{2}\right)^{n+2}(3t-3r-1)(6n-3t+3r+1), & \text{if } r = \text{odd}, t = \text{even;} \\ \left(\frac{1}{2}\right)^{n+2}(3t-3r+1)(6n-3t+3r-1), & \text{if } r = \text{even}, t = \text{odd.} \end{cases}$$

So,

$$\begin{aligned} \sum_{n+1 \leq j < k \leq 3n} \det(-L_R(\{j, k\}|\{j, k\})) &= (-4)^n \left(\frac{1}{2}\right)^{n+2} \left\{ \sum_{\substack{1 \leq r < t \leq 2n \\ \{r, t\} = \{\text{even or odd}\}}} 9(t-r)(2n-t+r) \right. \\ &+ \sum_{\substack{1 \leq r < t \leq 2n \\ r-\text{odd}, t-\text{even}}} (3t-3r-1)(6n-3t+3r+1) \\ &+ \left. \sum_{\substack{1 \leq r < t \leq 2n \\ r-\text{even}, t-\text{odd}}} (3t-3r+1)(6n-3t+3r-1) \right\} \\ &= (-4)^n \left(\frac{1}{2}\right)^{n+2} \{6n(n^2-1) + (n-1)(3n^2+n+2) + (n+1)(3n^2-n+2)\} \\ &= (-4)^n \left(\frac{1}{2}\right)^n n^2(3n^2-1). \end{aligned}$$

Case A5. Suppose that $1 \leq j \leq n$ and $n+1 \leq k \leq 3n$. In such a case, we have that $\sum_{\substack{1 \leq j < n \\ n+1 \leq k \leq 3n}} \det(-L_R(\{j, k\}|\{j, k\})) = \begin{vmatrix} -4I_{n-1} & V \\ V^T & \chi(\{k\}|\{k\}) \end{vmatrix}$, where V is a submatrix of $-\sqrt{2}L_{01}$ created by removing the j th row and k th column of $-\sqrt{2}L_{01}$. Taking $t = k - n$, we can compute $\det(\chi(\{t\}|\{t\}) + \frac{1}{2}V^TV)$:

$$\left\{ \begin{array}{ll} \frac{(-1)^{n-1}(36(-j^2+iq+in)-9(t^2+2qn)+8(6j-3t-3n-2))}{2^{n+1}}, & \text{if } j > 1, t < 2j - 2 \text{ and even;} \\ \frac{(-1)^{n-1}(36(-j^2+iq+in)-9(t^2+2qn)+30(2j-t-n-1)+5)}{2^{n+1}}, & \text{if } j > 1, 1 < t < 2j - 2 \text{ and odd;} \\ \frac{(-1)^{n-1}(36(-j^2+iq-in)-9(t^2+2qn)+8(6j-3qn-3n-2))}{2^{n+1}}, & \text{if } j > 1, 2n > t > 2j - 2 \text{ and even;} \\ \frac{(-1)^{n-1}(36(-j^2+iq-in)-9(t^2+2qn)+30(2j-qn-n-1)+5)}{2^{n+1}}, & \text{if } j > 1, t > 2j - 1 \text{ and odd;} \\ \frac{(-1)^{n-1}(9(2nq-t^2)+6(t-n)-1)}{2^{n+1}}, & \text{if } j = 1, t = \text{odd;} \\ \frac{(-1)^{n-1}(9(2nq-t^2)+12(t-n)-4)}{2^{n+1}}, & \text{if } j = 1, t = \text{even;} \\ \frac{(-1)^{n-1}(3n-1)}{2^{n-1}}, & \text{if } j > 1, t = 2j - 1 \text{ or } 2j - 2; \\ \frac{(-1)^{n-1}(9(ni-j^2)+4(6j-3n-4))}{2^{n-1}}, & \text{if } j > 1, t = 1; \\ \frac{(-1)^{n-1}(9(ni-j^2)+6(2j-n)-4)}{2^{n-1}}, & \text{if } j > 1, t = 2n. \end{array} \right.$$

We have

$$\sum_{\substack{1 \leq j < n \\ n+1 \leq k \leq 3n}} \det(-L_R(\{j, k\}|\{j, k\})) = -(-4)^{n-1} \left(\frac{1}{2}\right)^{n-1} n^2(3n^2+1).$$

Thus,

$$\begin{aligned} \alpha_{3n-2} &= \sum_{1 \leq j < k \leq 3n} \det(-L_R(\{j, k\}|\{j, k\})) = \sum_{1 \leq j < k \leq n} \det(-L_R(\{j, k\}|\{j, k\})) \\ &+ \sum_{n+1 \leq j < k \leq 3n} \det(-L_R(\{j, k\}|\{j, k\})) + \sum_{\substack{1 \leq j < n \\ n+1 \leq k \leq 3n}} \det(-L_R(\{j, k\}|\{j, k\})) \\ &= (-4)^{n-2} \left(\frac{1}{2}\right)^n 3n^2(n^2-1) + (-4)^n \left(\frac{1}{2}\right)^n (3n^4-n^2) \\ &+ (-4)^{n-1} \left(\frac{1}{2}\right)^{n-1} n^2(3n^2+1) \\ &= -2^n n^2 \frac{15(75n^2-11)}{16}. \quad \square \end{aligned}$$

References

1. Spitzer, F. *Principles of Random Walk*; Springer Science and Business Media: Berlin/Heidelberg, Germany, 2013.
2. Perozzi, B.; Al-Rfou, R.; Skiena, S. Deepwalk: Online learning of social representations. In Proceedings of the 20th ACM SIGKDD International Conference on Knowledge Discovery and Data Mining (ACM), New York, NY, USA, 24–27 August 2014; pp. 701–710.
3. Yang, X.S.; Deb, S. Multi-objective cuckoo search for design optimization. *Comput. Oper. Res.* **2013**, *40*, 1616–1624. [[CrossRef](#)]
4. Adhikari, R.; Agrawal, R.K. A combination of artificial neural network and random walk models for financial time series forecasting. *Neural Comput. Appl.* **2014**, *24*, 1441–1449. [[CrossRef](#)]
5. Verstraete, F.; Wolf, M.M.; Cirac, J.I. Quantum computation and quantum-state engineering driven by dissipation. *Nat. Phys.* **2009**, *5*, 633–636. [[CrossRef](#)]
6. Codling, E.A.; Plank, M.J.; Benhamou, S. Random walk models in biology. *J. R. Soc. Interface* **2008**, *5*, 813–834. [[CrossRef](#)] [[PubMed](#)]
7. Mei, Q.; Zhou, D.; Church, K. Query suggestion using hitting time. In Proceedings of the 17th ACM Conference on Information and Knowledge Management (ACM), NapaValley, CA, USA, 26–30 October 2008; pp. 469–478.
8. Boccaletti, S.; Latora, V.; Moreno, Y.; Chavez, M.; Hwang, D.U. Complex networks: Structure and dynamics. *Phys. Rep. Rev. Sect. Phys. Lett.* **2006**, *424*, 175–308. [[CrossRef](#)]
9. Redner, S. *A Guide to First-Passage Processes*; Cambridge University Press: Cambridge, UK, 2001.
10. Polizzi, N.F.; Therien, M.J.; Beratan, D.N. Mean first-passage times in biology. *Isr. J. Chem.* **2016**, *56*, 816. [[CrossRef](#)] [[PubMed](#)]
11. Metzler, R.; Oshanin, G.; Redner, S. *First-Passage Phenomena and Their Applications*; World Scientific: Singapore, 2014.
12. Xie, Y.Y.; Chang, S.H.; Zhang, Z.P.; Zhang, M.; Yang, L. Efficient sampling of complex network with modified random walk strategies. *Phys. A Stat. Mech. Appl.* **2018**, *492*, 57–64. [[CrossRef](#)]
13. Kemeny, G.; Snell, J.L. *Finite Markov Chains*; Van Nostrand: Princeton, NJ, USA, 1960.
14. Van Mieghem, P. *Graph Spectra for Complex Networks*; Cambridge University Press: Cambridge, UK, 2011.
15. Zhu, H.Y.; Klein, D.J.; Lukovits, I. Extensions of the Wiener number. *J. Chem. Inf. Comput. Sci.* **1996**, *36*, 420–428. [[CrossRef](#)]
16. Gutman, I.; Mohar, B. The quasi-Wiener and the Kirchhoff indices coincide. *J. Chem. Inform. Comput. Sci.* **1996**, *36*, 982–985. [[CrossRef](#)]
17. Chandra, A.K.; Raghavan, P.; Ruzzo, W.L.; Smolensky, R. The electrical resistance of a graph captures its commute and cover times. In Proceedings of the Twenty-First Annual ACM Symposium on Theory of Computing, Edmonton, AB, Canada, 14–16 August 1989; pp. 574–586.
18. Levene, M.; Loizou, G. Kemeny’s constant and the random surfer. *Am. Math.* **2002**, *109*, 741–745. [[CrossRef](#)]
19. Xiao, W.; Gutman, I. Resistance distance and Laplacian spectrum. *Theor. Chem. Acc.* **2003**, *110*, 284–289. [[CrossRef](#)]
20. Zhang, Z.; Wu, B.; Zhang, H.; Zhou, S.; Guan, J.; Wang, Z. Determining global mean-first-passage time of random walks on Vicsek fractals using eigenvalues of Laplacian matrices. *Phys. Rev. E* **2010**, *81*, 031118. [[CrossRef](#)] [[PubMed](#)]
21. Zaman, S.; Ullah, A. Kemeny’s constant and global mean first passage time of random walks on octagonal cell network. *Math. Methods Appl. Sci.* **2023**, *46*, 91779186. [[CrossRef](#)]
22. Ali, U.; Ahmad, Y.; Xu, S.A.; Pan, X.F. Resistance distance-based indices and spanning trees of linear pentagonal-quadrilateral networks. *Polycycl. Aromat. Compd.* **2021**, *42*, 6352–6371. [[CrossRef](#)]
23. Ali, U.; Raza, H.; Ahmed, Y. On normalized Laplacians, degree-Kirchhoff index and spanning tree of generalized phenylene. *Symmetry* **2021**, *13*, 1374. [[CrossRef](#)]
24. Zhang, X.; Awais, H.M.; Javaid, M.; Siddiqui, M.K. Multiplicative Zagreb indices of molecular graphs. *J. Chem.* **2019**, *2019*, 5294198. [[CrossRef](#)]
25. Ullah, A.; Zeb, A.; Zaman, S. A new perspective on the modeling and topological characterization of H-Naphtalenic nanosheets with applications. *J. Mol. Model.* **2022**, *28*, 211. [[CrossRef](#)]
26. Kosar, Z.; Zaman, S.; Siddiqui, M.K. Structural characterization and spectral properties of hexagonal phenylene chain network. *Eur. Phys. J. Plus* **2023**, *138*, 415. [[CrossRef](#)]
27. Zaman, S. Spectral analysis of three invariants associated to random walks on rounded networks with $2n$ -pentagons. *Int. J. Comp. Math.* **2022**, *99*, 465–485. [[CrossRef](#)]
28. Ali, U.; Li, J.; Ahmad, Y.; Raza, Z. Computing the Laplacian spectrum and Wiener index of pentagonal-derivation cylinder/Möbius network. *Heliyon* **2024**, *10*, e24182. [[CrossRef](#)]
29. Došlic, T.; Måloy, F. Chain hexagonal cacti: Matchings and independent sets. *Discrete Math.* **2010**, *310*, 1676–1690. [[CrossRef](#)]
30. Chen, X.; Zhao, B.; Zhao, P. Six-membered ring spiro chains with extremal Merrifield-Simmons index and Hosoya index. *Match Commun. Math. Comput. Chem.* **2009**, *62*, 657–665.
31. Huang, J.; Li, S.C.; Li, X.C. The normalized Laplacian degree-Kirchhoff index and spanning trees of the linear polyomino chains. *Appl. Math. Comput.* **2016**, *289*, 324–334. [[CrossRef](#)]
32. Zhang, F. (Ed.) *The Schur Complement and Its Applications*; Springer: New York, NY, USA, 2005.

Disclaimer/Publisher’s Note: The statements, opinions and data contained in all publications are solely those of the individual author(s) and contributor(s) and not of MDPI and/or the editor(s). MDPI and/or the editor(s) disclaim responsibility for any injury to people or property resulting from any ideas, methods, instructions or products referred to in the content.